

Increasing the bandwidth of High Harmonic Generation emission peaks by spectrally splitting and recombining the driver field

Eldar Ragonis^{1,2}, Eran Ben Arosh^{1,2}, Lev Merensky^{1,2} and Avner Fleischer^{1,2*}

¹ *Raymond and Beverly Sackler Faculty of Exact Sciences, School of Chemistry, Tel Aviv University, Tel Aviv 6997801, Israel*

² *Tel-Aviv University center for Light-Matter-Interaction, Tel Aviv 6997801, Israel*

**Corresponding Author: avnerfleisch@tauex.tau.ac.il*

Abstract

We demonstrate a High-Harmonic-Generation (HHG) scheme which generates a dense spectrum rather than a sparse one, without the use of short driver pulses. The scheme uses a two-color driver with close frequencies, resulting in the generation of new emission channels which coalesce into broad peaks, the bandwidth of which increases with photon energy. Liberated from conversion losses and complexities associated with the generation of short driver pulses, this source will find use in HHG applications benefiting from high-flux broadband extreme ultra violet (XUV) radiation such as attosecond transient absorption spectroscopy.

PACS numbers: 42.65.Ky, 42.65.Re

High Harmonic Generation (HHG) offers a key tabletop source of radiation in the extreme ultra violet (XUV) regime, important for many applications ranging from studies in attosecond science and time-resolved studies of ultrafast electron dynamics in matter [1-3] to imaging of nanostructures [4-6]. Driving the process by a quasi-monochromatic driver results in the emission of a sparse comb of odd-integer multiples of the driver frequency. Many applications however require XUV radiation at wavelengths which do not coincide with the peaks in the comb. For instance, in attosecond transient absorption spectroscopy (ATAS) [7-9] the time-dependent absorption of the XUV radiation in matter is studied, and a sparse XUV source might give only partial information of the dynamical process taking place. The most frequently-used solution to overcome this difficulty is to reduce the number of induced electron recollisions, by shortening the duration of the driver pulses. This not only broadens the width of each peak in the comb but also generates a broad supercontinuum at the cutoff energy of the spectrum. Nevertheless, even with this method the HHG spectra (HGS) still exhibits low spectral content around even-integer multiples of the driving frequency in the plateau region.

Few- (possibly single-) cycle driver pulses are most commonly generated by the well-established method of spectrally broadening intense femtosecond-pulses in a gas-filled hollow-core capillary (HCF) [10], followed by subsequent pulse-compression in multilayer chirped mirrors. Several drawbacks are however associated with this method. First, the damage threshold of the glass capillary restricts the input beam average power to less than few Watts (see [11] and references therein), that is to few milijoules per pulse at repetition rates up to 10kHz or so (coupling of higher average power lasers has also been demonstrated, but with hundred-fs-duration input pulses [12-13]). Second, this method is lossy as the transmission efficiency of the HCF, frequency-conversion losses due to self-phase modulation (SPM), absorption and the finite reflectivity of the chirped mirrors all limit the power of the generated short pulses to about half of that of the input beam. Third, the beam profile exiting the HCF is spectrally inhomogeneous as the amount of self-phase modulation experienced is maximal at the axis of the capillary and decreases with the radial direction. All the above complicate the use of this method with very high average-power laser sources (due to the thermal load and resulting instabilities), or with low-power sources for which either 50% throughput is unacceptable or the spectral broadening is insufficient.

Here we present a HHG scheme to generate dense (rather than sparse) HGS, with increased bandwidth of each

harmonic peak, without relying on short driver pulses. In the method driver pulses, such as the ones delivered by a commercial amplified Ti:Sa laser are spectrally split and recombined to generate a two-color driver with close central wavelengths, slightly above and below the central wavelength of the Ti:Sa pulses. This is achieved by feeding the input Ti:Sa pulses into an interferometer where the common spectrally-flat beamsplitters are replaced by hard-edge shortpass dichroic mirrors with a cutoff wavelength close to the central wavelength of the Ti:Sa pulses. After combining the beams they are spatially and temporally overlapped. Driving HHG using this driver turns the HHG scheme into a bichromatic one. This considerably broadens the peaks in the HGS, which with increasing XUV photon energy could coalesce, yielding a practically continuous HGS. With this method substantial HHG spectral content is obtained which can be even tuned around even-integer multiples of the input driver's frequency. The method is simple and economic, and with perfect hard-edge dichroics it has no power losses as no power is wasted to the dump port of the interferometer.

Let us now elaborate on the mechanism behind the proposed HHG scheme. Suppose for simplicity that the input pulses entering the interferometer have a Gaussian spectrum profile $S(\omega) = \exp[-a(\omega - \omega_0)^2]$ and that the spectrum's width is narrow enough such that the spectral content at zero frequency is negligible (i.e., $a\omega_0^2 \gg 1$). Then the pulse's central frequency is given by

$$\langle \omega \rangle = \frac{\int_0^{\infty} d\omega \omega S(\omega)}{\int_0^{\infty} d\omega S(\omega)} = \omega_0 \quad (1)$$

When this input pulse is used as a driver in HHG, the generated harmonics are odd-integer multiples of the driver's central frequency $\Omega = (2n - 1)\omega_0$ (n is an integer). The spectral width of each harmonic is inversely-proportional to the number of electron recollisions occurring in the process, which is determined by the driver's spectral width. Suppose this pulse enters the interferometer where the dichroic mirrors spectrally split (and later recombine) the pulse at its central frequency ω_0 . Then two pulses exit the interferometer, the central frequency of each being:

$$\omega_1 \equiv \frac{\int_{\omega_0}^{\infty} d\omega \omega S(\omega)}{\int_{\omega_0}^{\infty} d\omega S(\omega)} = \omega_0 + \sqrt{\frac{1}{\pi a}} \quad (2)$$

and

$$\omega_2 \equiv \frac{\int_0^{\omega_0} d\omega \omega S(\omega)}{\int_0^{\omega_0} d\omega S(\omega)} = \omega_0 - \sqrt{\frac{1}{\pi a}} \quad (3)$$

When the two pulses are overlapped in time, a two-color field is obtained. When this field is used to drive HHG, the following harmonic emission channels are obtained [14]:

$$\begin{aligned} \Omega_{(n_1, n_2)} &= n_1 \omega_1 + n_2 \omega_2, \quad n_1 + n_2 = 2n - 1 \\ &= (n_1 + n_2) \omega_0 + (n_1 - n_2) \sqrt{\frac{1}{\pi a}} \end{aligned} \quad (4)$$

Where n_1, n_2 are integers which refer to the number of annihilated photons from each color ω_1, ω_2 composing the driver. Hence, this simple procedure of spectrally splitting-and-recombining the input pulse generates additional HHG peaks $(n_1 - n_2) \sqrt{\frac{1}{\pi a}}$, controllable by the value of a . In particular, when a is large (this is obtained

when the bandwidth of the input pulse is small), i.e., the two frequencies ω_1, ω_2 are close, the spacing between each two peaks is small, which leads to dense HGS in the vicinity of the odd-harmonic frequencies. In general, the $(2n-1)^{\text{th}}$ harmonic (in terms of the input pulse central frequency ω_0) that would have been obtained were the HHG process driven by the input pulses, splits into the following set of $2n$ channels $\Omega_{(0,2n-1)}, \dots, \Omega_{(n,n-1)}, \Omega_{(n+1,n-2)}, \Omega_{(n+2,n-3)}, \dots, \Omega_{(2n-1,0)}$ when driven by the bichromatic driver. This set covers the energies $(2n-1)\omega_0 - (2n-1)\sqrt{\frac{1}{\pi a}}$ to $(2n-1)\omega_0 + (2n-1)\sqrt{\frac{1}{\pi a}}$. Clearly, the bandwidth covered by all these peaks increases at high harmonic orders (large n). The channels emerging from adjacent odd harmonics may even get nested one into another such that for any practical purposes a supercontinuum is obtained. Moreover, increasing the bandwidth of the input pulses (small a) increases the difference between the central frequencies of the 2 arms $\omega_1 - \omega_2$, which make the HGS less sparse as the harmonic peaks are more spread over the bandwidth of the emission.

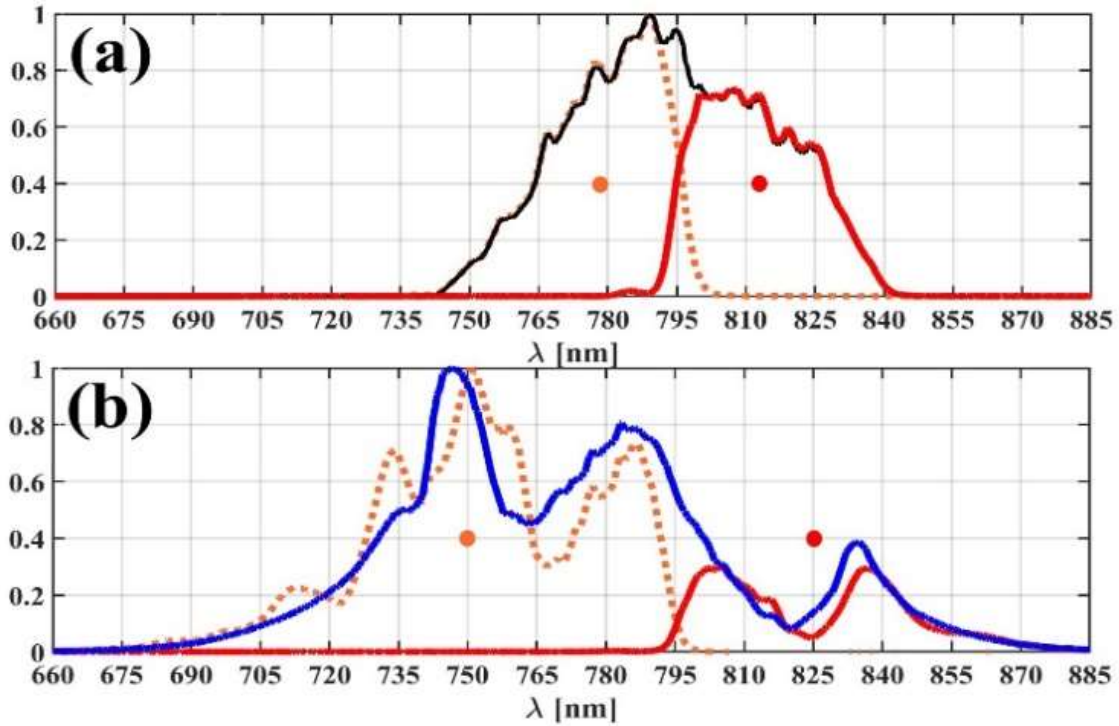


Fig. 1. (a) spectrum of the Ti:Sa laser pulses entering the interferometer (black) and exiting the interferometer (arm 1- dashed orange, arm 2- solid red). (b) spectrum of the broadened Ti:Sa laser pulses after the HCF (blue) and exiting the interferometer (arm 1- dashed orange, arm 2- solid red). The dichroic mirrors cutoff wavelength is at 795nm. The orange and red dots indicate the central wavelength λ_1, λ_2 of the pulses from arms 1 and 2, respectively.

In our experiment we use a commercial amplified Ti:Sa laser (Legend-Elite Duo HE+USX-5kHz by *Coherent*) which delivers linearly-polarized (horizontal, “p”-polarization) 25fs, 3mJ pulses at repetition rate of 5kHz. Half of that beam is used for our experiment. The laser pulses are spectrally split and recombined in a Mach-Zehnder interferometer whose spectrally-flat beamsplitters were replaced with hard-edge short-pass dichroic mirrors. The dichroic mirrors have a cutoff wavelength at 795nm, around the central wavelength of the Ti:Sa pulses. The interferometer generates two pulses out of each incoming Ti:Sa pulse, with central wavelengths of $\lambda_1 = 778\text{nm}$

and $\lambda_2 = 812\text{nm}$, respectively. The spectra of the input field and the two exit fields are shown in Fig.1a. After combining the beams they are spatially and temporally overlapped (one arm of the interferometer is placed on a motorized linear stage), forming the two-color driver. In order to add controllability to this bichromatic HHG scheme, the polarization degree of freedom [14] is utilized by adding two elements. First, a super-achromatic half waveplate (B. Halle) is placed in arm 1 of the interferometer, and flips the linear polarization from horizontal (“p”) to vertical (“s”). Second, at the exit of the interferometer, before entering the HHG generation chamber, the combined beam passes through a super-achromatic quarter-waveplate (B. Halle) placed on a motorized rotation stage. As we will show, the reading of this waveplate α controls the HGS obtained, as the possible emission channels are dictated by spin angular momenta conservation law. In our setup $\alpha = 0^0$ corresponds to cross-orthogonal linear-polarizations of the two colors, and $\alpha = \pm 45^0$ corresponds to a bicircular counter-rotating driver (the two colors are circularly-polarized with opposite helicities). An intermediate value, i.e., $\alpha = -30^0$ corresponds to bielliptical counter rotating driver, with orthogonal major axes of the polarization ellipses of the two colors.

Using Second harmonic-generation Frequency-Resolved Optical Gating (SHG-FROG) the pulse durations from each arm just prior to the HHG chamber entrance window were measured to be 45fs and 55fs respectively, with slight chirp (quadratic phase). The energy per pulse in each arm was $440\mu\text{J}$ and $480\mu\text{J}$ respectively. The two-color driver is focused (using a $f=750\text{mm}$ focusing mirror) onto an Argon jet and the resulting XUV radiation is filtered from the remaining infra-red driver radiation with a $0.2\mu\text{m}$ -thick Aluminum foil. It then enters a home-built HHG spectrometer composed of an entrance slit of $50\mu\text{m}$, aberration-corrected flat-field concave grating with 300 lines/mm (30-006 by *Shimadzu*), and a back-illuminated CCD camera (Newton DO940P-BN by *Andor*). The spectrometer has a typical resolution of 25meV at 30eV and 90meV at 70eV . The spectrometer components reside on a breadboard which is attached to the optical table. All are isolated from the chamber enclosure by means of flexible edge-welded bellows., in order to decouple the optical setup from possible vibrations induced by the turbo pumps.

Fig. 2a shows the obtained HGS as function of harmonic order (in units of the frequency ω_0) and the quarter-waveplate reading α . For $\alpha = \pm 45^0$ the driver is bicircular and counter-rotating. Spin angular momenta conservation considerations dictate that only two harmonic channels are possible in this setting: $\Omega_{(n-1,n)}, \Omega_{(n,n-1)}$. These channels are circularly-polarized with opposite helicities. As the reading α increases, more channels become allowed because a driver with elliptical polarization supplies the system with circularly-polarized photons of the two possible opposite helicities.. In fact, in the basis of circular polarization, each channel is characterized by four integers $(n_1^+, n_1^-, n_2^+, n_2^-)$ which refer to the number of annihilated photons from arm 1 (2) and positive (negative) helicity, respectively. The energy and spin state of harmonic channel $(n_1^+, n_1^-, n_2^+, n_2^-)$ are respectively $\Omega_{(n_1^+, n_1^-, n_2^+, n_2^-)} = (n_1^+ + n_1^-)\omega_1 + (n_2^+ + n_2^-)\omega_2$ and $\sigma_{(n_1^+, n_1^-, n_2^+, n_2^-)} = (n_1^+ + n_2^+) - (n_1^- + n_2^-)$. Hence, the two channels obtained for $\alpha = -45^0$ are $\Omega_{(n-1,0,0,n)}, \Omega_{(n,0,0,n-1)}$ and for $\alpha = 45^0$ are $\Omega_{(0,n-1,n,0)}, \Omega_{(0,n,n-1,0)}$. As α approaches zero, circular photons of both helicities are formed in the driver, enabling the appearance of higher- and lower- energy channels, e.g. as in the diagram in Fig.3. Note that in this diagram the vertical axis represents the energy of the photonic channel and the horizontal axis is in proportion to the reading α and indicates the number of new circular driver photons n_1^-, n_2^+ . At $\alpha = 0^0$ the maximal number of channels is allowed, extending all the way from $\Omega_{(0,0,n-1,n)}, \Omega_{(0,0,n,n-1)}$ to $\Omega_{(n,n-1,0,0)}, \Omega_{(n-1,n,0,0)}$. At this setting the emission support is the largest since the maximal number of channels is allowed. This is evident also from Fig.2b in which lineouts from Fig. 2a are shown. Although the emission is still peaked around odd-integer multiples of ω_0 , the technique of spectrally splitting and recombining the driver pulse allows the bandwidth of each odd-integer peak to be increased 5-fold, As α is changed from $\alpha = -45^0$ to $\alpha = 0^0$.

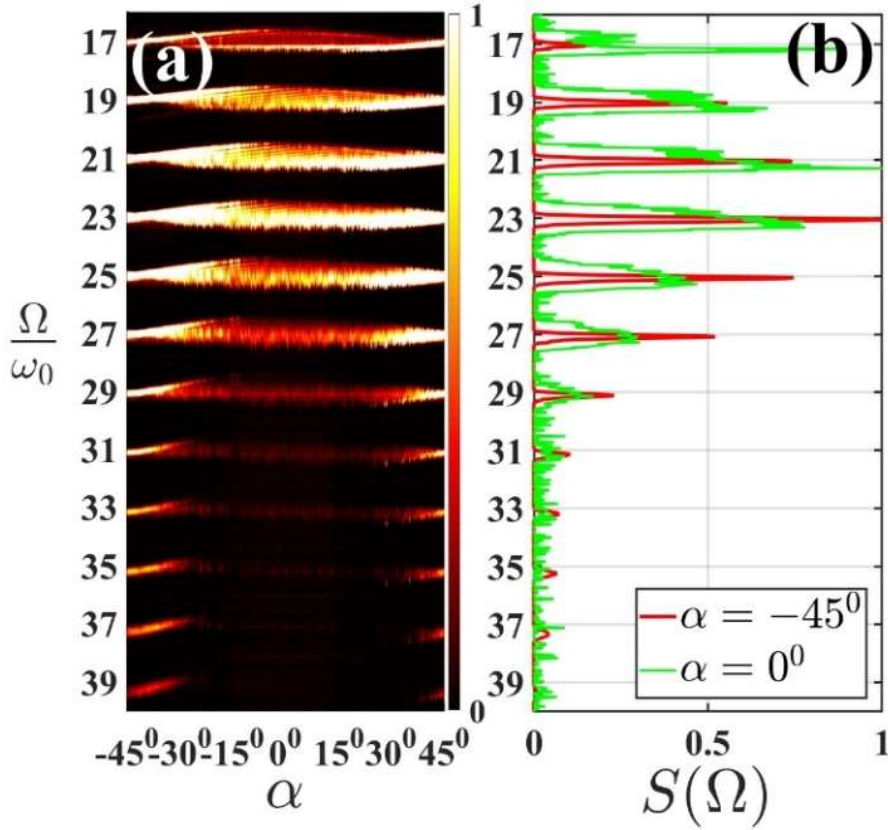


Fig. 2. (a) HGS intensity (linear scale, normalized to 60000counts/sec) vs. harmonic order and angle α of the achromatic quarter waveplate; The spectrum of the two-color driver which exits the interferometer is given in by the orange and red curves of Fig. 1(a). For $\alpha = 0^\circ$ the fields are perpendicularly-linearly polarized and for $\alpha = \pm 45^\circ$ they are counter-rotating bicircularly polarized. (b) HGS lineouts from (a) at $\alpha = -45^\circ$ (red curve) and $\alpha = 0^\circ$ (green curve).

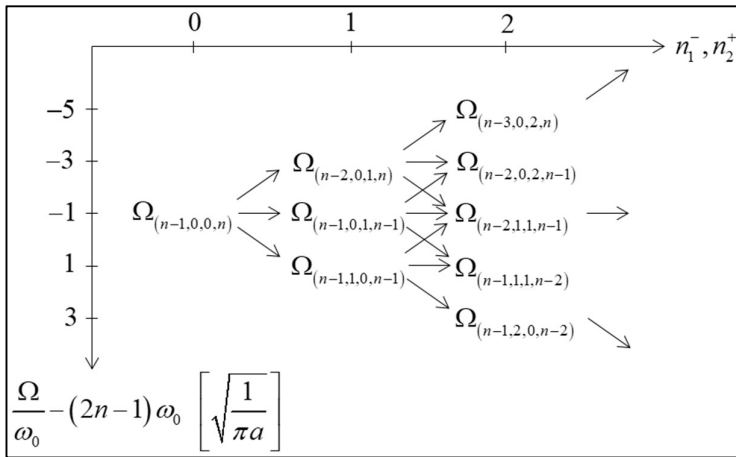


Fig. 3. Diagram representing the birth of harmonic channels as the quarter waveplate reading increases from $\alpha = -45^\circ$. The horizontal axis counts the number of new photons n_1^-, n_2^+ which the driver can supply to the HHG process when the quarter waveplate is rotated. These photons give rise to new harmonic channels. The vertical axis represents the energy of the photonic channels in units of the detuning $\sqrt{\frac{1}{\pi\alpha}}$.

Next, we present results in which the harmonic spectral support is increased even further. We feed the interferometer with input pulses with a slightly larger bandwidth. This is done by moderately spectrally-broadening the Ti:Sa input pulses in a 1m-long HCF with inner diameter 500 μm , filled with 800mbar of Neon. The beam then bounces several times on chirped mirrors (PC70 by *Ultrafast Innovations*) until short pulses (11fs) are obtained. The two driver pulses exiting the interferometer now have central wavelengths of $\lambda_1 = 752\text{nm}$ and $\lambda_2 = 825\text{nm}$, respectively. The pulse duration from each arm was 16fs and 28fs respectively, with about 10% of the intensity present in satellite-pulses. The energy per pulse was 150 μJ in each of the two arms. As is evident from Fig.4, increasing the difference between the central frequencies of the 2 arms $\omega_1 - \omega_2$, extends the span of harmonic channels such that channels emerging from adjacent odd-integer values $(2n-1)$ get nested one into another to the extent that for any practical purposes a supercontinuum is obtained for $-25^\circ < \alpha < 25^\circ$. For comparison, driving HHG directly with the short 11 fs driver pulses yields bandwidth of roughly half an harmonic order (0.6eV) for each odd harmonic peak. Hence, with our technique the bandwidth of each harmonic peak increases 5-fold, in accordance with the results presented in Fig.2. It should be noted that in both Fig. 2a and Fig.4a as α is varied, each group of channels emerging from an odd-integer harmonic $(2n-1)$ forms a structure of n tilted lines. The origin of these lines is beyond the scope of this manuscript and will be described in a future publication [15].

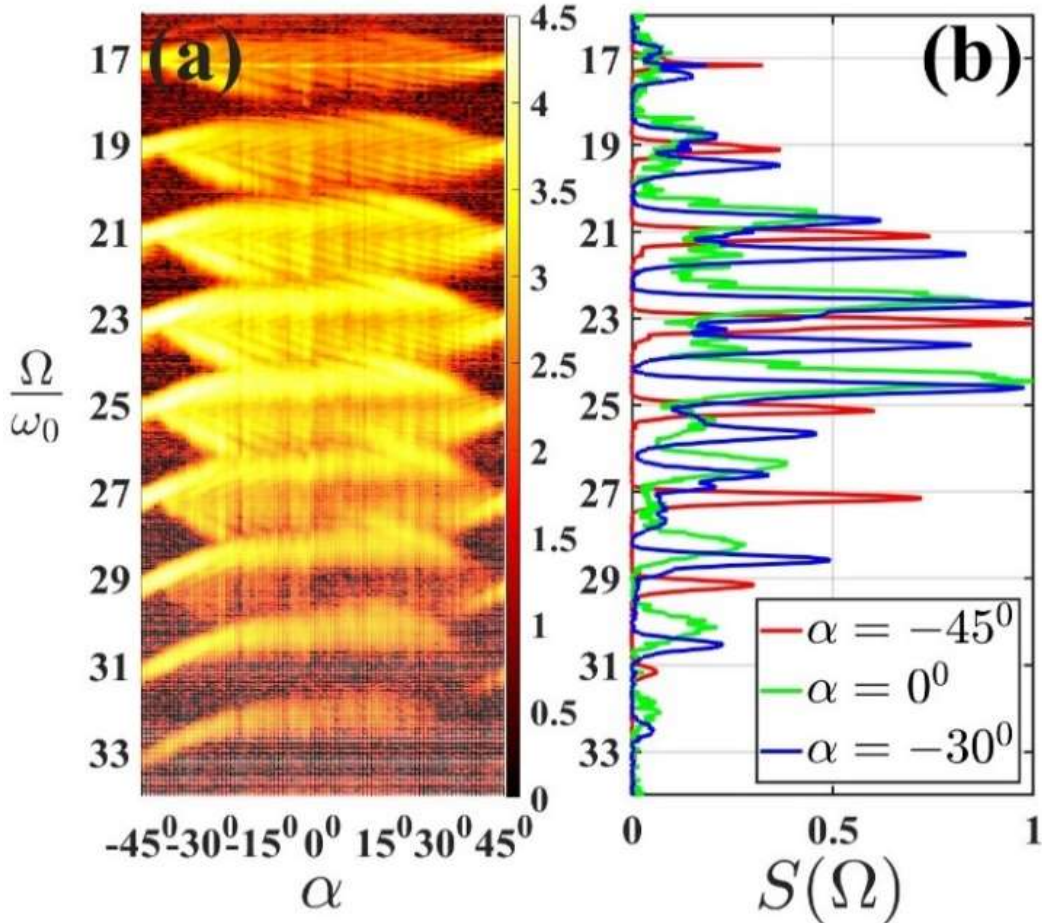


Fig. 4. (a) HGS intensity (logarithmic scale, maximal reading corresponds to 60000counts/sec) vs. harmonic order and angle α of the achromatic waveplate; The spectrum of the two-color driver which exits the interferometer is given in by the orange and red curves of Fig. 1(b). (b) HGS lineouts from (a) at $\alpha = -45^\circ$ (counter-rotating circularly polarized drivers, red curve), $\alpha = 0^\circ$ (perpendicularly-linearly polarized drivers, green curve), $\alpha = -30^\circ$ (perpendicularly-elliptically polarized drivers, blue curve).

To summarize, we have described a simple method to increase the bandwidth of harmonic peaks 5-fold, without using short driver pulses. Instead, the driver needs to be spectrally split and recombined in an interferometer with hard-edge dichroic mirrors. In principle, this procedure should impose no losses. Since it is also free of the losses accompanying the typical method of short driver pulse generation by SPM in a HCF it offers the potential for power scaling without losses. This makes the proposed scheme especially suited for use with high average-power lasers at large laser facilities.

Funding. Israel Science Foundation (524/19).

Acknowledgments. We thank Prof. Oren Cohen and Dr. Pavel Sidorenko for assistance with the FROG Ptychographic retrieval algorithm (<https://oren.net.technion.ac.il/ptych-frog/>).

Disclosures. The authors declare no conflicts of interest.

Data availability. Data underlying the results presented in this paper may be obtained from the authors upon reasonable request.

References

1. P. Corkum and F. Krausz, "Attosecond Science", *Nat. Phys.* **3** 381-387 (2007).
2. F. Krausz and M. Ivanov, "Attosecond Physics", *Rev. Mod. Phys.* **81** 545 (2009).
3. J. Li, J. Lu, A. Chew, S. Han, J. Li, Y. Wu, H. Wang, S. Ghimire and Z. Chang, "Attosecond science based on high harmonic generation from gases and solids", *Nat. Comm.* **11** 2748 (2020).
4. O. Kfir, S. Zayko, C. Nolte, M. Sivilis, M. Möller, B. Hebler, S. S. P. K. Arekapudi, D. Steil, S. Schäfer, M. Albrecht, O. Cohen, S. Mathias and Claus Ropers, "Nanoscale magnetic imaging using circularly polarized high-harmonic radiation." *Science advances* **3.12** (2017): eaao4641.
5. J. Miao, T. Ishikawa, I. K. Robinson, M. M. Murnane, "Beyond crystallography: Diffractive imaging using coherent X-ray light sources," *Science* **348**, 530 (2015).
6. E. R. Shanblatt, C. L. Porter, D. F. Gardner, G. F. Mancini, R. M. Karl, Jr., M. D. Tanksalvala, C. S. Bevis, V. H. Vartanian, H. C. Kapteyn, D. E. Adams, and M. M. Murnane, "Quantitative Chemically Specific Coherent Diffractive Imaging of Reactions at Buried Interfaces with Few Nanometer Precision", *Nano Lett.* **16** 5444 (2016).
7. R. Geneaux, H. J. B. Marroux, A. Guggenmos, D. M. Neumark and S. R. Leone, "Transient absorption spectroscopy using high harmonic generation: a review of ultrafast X-ray dynamics in molecules and solids" *Philosophical Transactions of the Royal Society A* **377** 20170463 (2019).
8. H. Wang, M. Chini, S. Chen, C.-H. Zhang, F. He, Y. Cheng, Y. Wu, U. Thumm, and Z. Chang, "Attosecond Time-Resolved Autoionization of Argon", *Phys. Rev. Lett.* **105** 143002 (2010).
9. P. Peng, C. Marceau, M. Hervé, P.B. Corkum, A. Yu. Naumov and D. M. Villeneuve, "Symmetry of molecular Rydberg states revealed by XUV transient absorption spectroscopy", *Nat. Comm.* **10** 5269 (2019).
10. M. Nisoli, S. DeSilvestri and O. Svelto, "Generation of high energy 10 fs pulses by a new pulse compression technique. *Appl. Phys. Lett.* **68**, 2793 (1996).
11. M. Dörner-Kirchner, V. Shumakova, G. Coccia, E. Kaksis, B. E. Schmidt, V. Pervak, A. Pugzlys, A. Baltuška, M. Kitzler-Zeiler and P. A. Carpeggiani, "HHG at the Carbon K-Edge Directly Driven by SRS Red-Shifted Pulses from an Ytterbium Amplifier", *ACS Photonics* **10** 84 (2023).
12. T. Nagy, T. Nagy, S. Hädrich, P. Simon, A. Blumenstein, N. Walther, R. Klas, J. Buldt, H. Stark, S. Breitschopf, P. Jójárt, I. Seres, Z. Várallyay, Eidam and J. Limpert, "Generation of three-cycle multi-millijoule laser pulses at 318 W average power", *Optica* **6** 1423 (2019).

13. D. Wilson, M. Ivanov, G. Tempea, A. Labranche, A. Ramirez, F. Légaré, C. Paradis, A. Hage, T. Mans, C. Trallero, B. E. Schmidt, “10mJ Hollow-Core Fiber operation at 250W average power with 90% efficiency”, CLEO: Science and Innovations, SM3O. 6 (Optica publishing group).
14. A. Fleischer, O. Kfir, T. Diskin, P. Sidorenko and O. Cohen, “Spin angular momentum and tunable polarization in high harmonic generation”, Nat. Photon. 8 543 (2014).
15. E. Ragonis, E. Ben-Arosh, L. Merensky and A. Fleischer, in preparation.